Single-Phase Self-Excited Induction Generator with Static VAR Compensator Voltage Regulation for Simple and Low Cost Stand-Alone Renewable Energy Utilizations Part I : Analytical Study

Tarek Ahmed*, Osamu Noro, Koji Soshin*, Shinji Sato*, Eiji Hiraki* and Mutsuo Nakaoka***

Abstract - In this paper, the comparative steady-state operating performance analysis algorithms of the stand-alone single-phase self-excited induction generator (SEIG) is presented on the basis of the two nodal admittance approaches using the per-unit frequency in addition to a new state variable defined by the per-unit slip frequency. The main significant features of the proposed operating circuit analysis with the per-unit slip frequency as a state variable are that the fast effective solution could be achieved with the simple mathematical computation effort. The operating performance results in the simulation of the single-phase SEIG evaluated by using the per-unit slip frequency state variable are compared with those obtained by using the per-unit frequency state variable. The comparative operating performance results provide the close agreements between two steady-state analysis performance algorithms based on the electro-mechanical equivalent circuit of the single-phase SEIG. In addition to these, the single-phase static VAR compensator; SVC composed of the thyristor controlled reactor; TCR in parallel with the fixed excitation capacitor; FC and the thyristor switched capacitor; TSC is applied to regulate the generated terminal voltage of the single-phase SEIG loaded by a variable inductive passive load. The fixed gain PI controller is employed to adjust the equivalent variable excitation capacitor capacitance of the single-phase SVC.

Keywords: single-phase self-excited induction generator, per-unit frequency nodal admittance approach, per-unit slip frequency nodal admittance approach, static VAR compensator, thyristor controlled reactor, thyristor switched capacitor, voltage regulation scheme for wind turbine power conditioner

1. Introduction

1.1 Equivalent Circuit of Single-Phase Induction Machine

Nowadays, the single-phase induction machine has been used widely in the fields of the automobile, transportation, industrial and consumer electrical drive applications as compared with the other kinds of the AC rotating machines. It is logical that the least expensive, the ruggedness, the smallest volumetric size, the lowest maintenance type of the AC machines should be used most often. In general, the single-phase induction machine is more suitable and acceptable for the cost effective machine in small-scale residential domestic utilizations. There are several types of the single-phase induction motors such as the split-phase and the shaded-pole in use today [1]. The equivalent circuit [1] of the aforementioned single-phase induction motor is shown in Fig.1 with the main winding of the stator supplied by the two or three wiring for the single-phase power source.

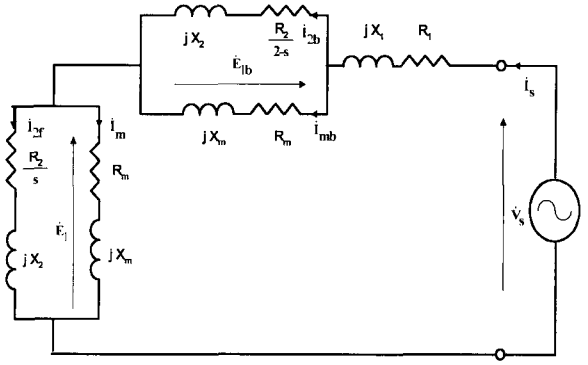

Fig.1 Equivalent circuit of single-phase induction motor

The slip; s is defined by $s=(N_S-N)/N_S$, N is the rotor shaft speed in rpm and Ns is the synchronous speed; N_S=1500 rpm when the supply frequency is 50Hz, R_1, X_1, R_2 and X_2 are the resistances and the leakage reactances of

* Dept. of Electrical and Electronic Engineering, Yamaguchi University, Japan. (tarek@pe-news1.eee.yamaguchi-u.ac.jp)
** Kawasaki Heavy Industry, Kobe, Japan
Received February 6, 2003; Accepted March 8, 2003.

the stator winding and the rotor winding referred to the stator winding side in ohm, respectively, X_m is the magnetizing reactance in ohm, R_m is the magnetizing reactance in ohm, and E_1, E_{1b}, V_s, I_s, I_{2f}, I_{2b}, I_{mb} and I_m are the air gap voltage due to the forward rotating field, the air gap voltage due to the backward rotating field, the single phase supply voltage, the supply current, the forward rotating field rotor current referred to the stator side, the backward rotating field rotor current referred to the stator side, the backward rotating magnetizing current and the magnetizing current of the forward rotating field of the single-phase induction machine, respectively.

1.2 Representation of Magnetization Characteristic of Single-Phase Induction Machine

The single-phase squirrel cage rotor type induction machine used for the feasible implementation has the following specifications; 4 poles 2 kW, 240 V, 15.7 A, 50 Hz, 1500 rpm. The induction machine parameters are estimated from the locked rotor test and the synchronous speed test of the single-phase induction machine as; R_1=1.4 ohm, X_1=2.1 ohm, R_2=0.59 ohm, and X_2=1.05 ohm. To determine the magnetization curve of the single-phase induction machine, the single-phase induction machine is driven at the synchronous speed N_S=1500 rpm and a variable AC supply voltage is applied to the stator winding at the rated frequency 50Hz[2-9]. According to the above conditions, the slip; s of the single-phase induction motor is equal to zero and hence the positive-sequence rotor branch ($R_2/s+jX_2$; s=0) in Fig.1 is equivalently opened. Also, the magnetizing reactance in the negative-sequence branch could be neglected as compared with the negative-sequence rotor branch (($R_2/(2-s)+jX_2$; s=0). Therefore, the magnetizing reactance X_m of the positive-sequence rotor branch is estimated by using the equivalent circuit shown in Fig.1,

$$X_m = \sqrt{(\frac{V_s}{I_S})^2 - (R_1 + R_m + \frac{R_2}{2})^2} - (X_1 + X_2) \quad (1)$$

where the experimental data of the supply voltage V_s against the supply current I_s is indicated in Fig.2. The positive-sequence air gap voltage E_1 is calculated by,

$$E_1 = I_s\sqrt{R_m^2 + X_m^2} \quad (2)$$

The relation between the positive-sequence air gap voltage E_1 and X_m is obtained experimentally and depicted in Fig.3. The magnetization curve obtained experimentally is represented by the following equation giving a sufficiently good mapping of the air gap rms voltage E_1 vs. the magnetizing reactance X_m curve using a piece-wise linear representation and given by,

$$E_1 = \begin{cases} 342.86 - 5.850X_m & X_m \le 22.69 \\ 450.00 - 3.773X_m & 22.69 \le X_m \le 25.77 \\ 871.43 - 26.860X_m & 25.77 \le X_m \le 27.12 \\ 0 & X_m \ge 27.12 \end{cases} \quad (3)$$

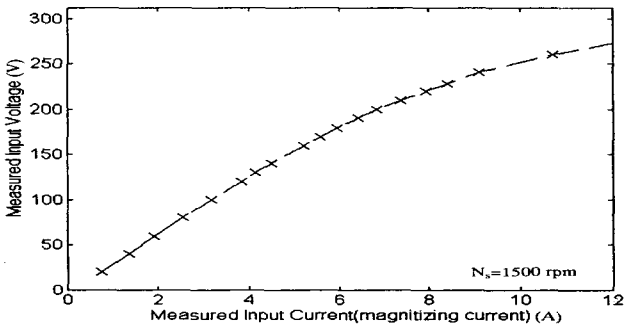

Fig. 2 Supply voltage against supply current of single-phase induction motor at no load

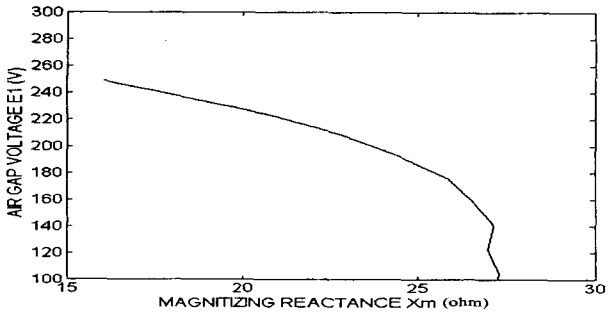

Fig. 3 Air gap voltage vs. magnetizing reactance of single-phase induction machine

1.3 Equivalent Circuit of Single-Phase Self-Excited Induction Generator

For power generation mode of the single-phase induction machine, the above equivalent circuit can be adapted by connecting an appropriate excitation capacitor in parallel with a certain stand-alone electrical passive load across the stator terminal ports of the single-phase induction machine instead of the single-phase power supply source as shown in Fig.4. In this case, the induction machine is driven by a mechanical prime mover.

Owing to the operation on an isolated network, the frequency of the output voltage can no longer be kept constant. The frequency variation affects to both the reactances and the value of the slip; s for a given speed. To take account of the frequency variation, all the reactances are represented in the per unit terms referred to the values meas-

ured at the base frequency 50 Hz, so that any reactance at a given frequency can be denoted by $X=f\,X_{base}$, where X is the reactance in ohm at the output frequency F of the single-phase SEIG, X_{base} is the reactance at 50 Hz and f=F/50 is the per unit frequency. By dividing all the equivalent circuit parameters and voltages denoted by f, the following equivalent circuit as illustrated in Fig.4 is obtained. In this circuit, the slip s is defined in terms of the per-unit frequency f and the relative rotor shaft speed υ where (υ=N/Ns), N is the mechanical rotor speed in rpm and Ns is the synchronous speed Ns =1500.0 rpm for 50Hz.

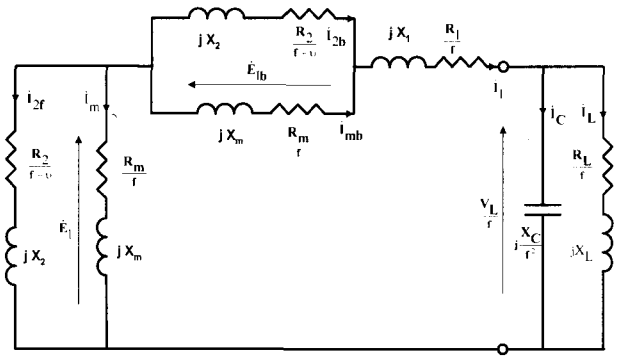

Fig. 4 Electro-mechanical equivalent circuit of single-phase SEIG

where R_L and X_L are the load resistance and reactance components in ohm, respectively. C is the excitation capacitor capacitance in farad. X_c is the excitation capacitive reactance in ohm (X_C=1/100πC; F=50Hz) and V_L, I_1, I_L and I_C are the output voltage, the stator current, the load current of the single-phase SEIG and the excitation current, respectively.

For only one paper presented previously [6], the approximate steady-state analysis in the frequency domain of the single-phase SEIG loaded by a resistive load has been done with the following assumptions

- Iron losses are negligible
- Only fundamental M.M.F. due to the forward rotating field waves are considered
- Resistances and inductances of the induction machine are constant, except for the magnetizing inductance described graphically by means of the magnetization curve.
- The rate of change in the parameters and variables of the equivalent circuit is extremely small, so that the steady-state equivalent circuit can be used. The electro-mechanical equivalent circuit of the single-phase SEIG based on the rated frequency is simplified and approximated to another one as depicted in Fig.5.

This paper presents comparative analytical studies by utilizing the nodal admittance approach to illustrate the operation of the single-phase SEIG in an isolated stand-alone operation along with the experimental evaluations. The steady-state operating performance calculations are described to support the frequency domain analysis. In addition, a closed loop PI compensator for the terminal voltage regulation of the single-phase SEIG driven directly by the wind turbine modeling represented by the separately-excited dc motor is established using the static VAR compensator; SVC composed of the thyristor phase controlled reactor; TCR in parallel with the thyristor switched capacitor; TSC and the fixed excitation capacitor FC connected to the single-phase SEIG with the passive electrical load.

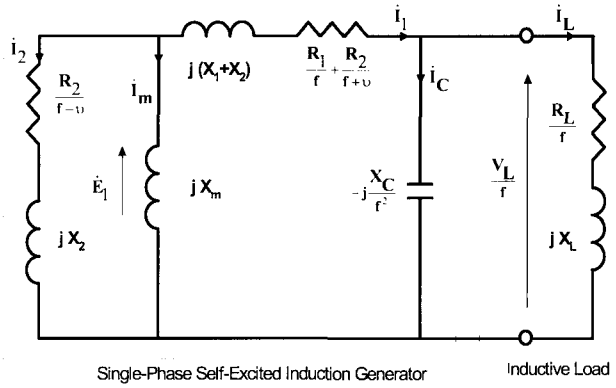

Fig. 5 Approximate electro-mechanical equivalent circuit of single-phase SEIG

2. Steady-State Operating Performance Analysis of Single-Phase SEIG

The equations representing the steady-state operating performance of the single-phase SEIG driven by the constant speed prime mover can be obtained by using the nodal admittance approach across the magnetizing branch in Fig.5, the following equation can be written as follows,

$$(\dot{Y}_e + \dot{Y}_m + \dot{Y}_r)\dot{E}_1 = 0 \tag{4}$$

where, $\dot{Y}_r$, $\dot{Y}_m$ and $\dot{Y}_e$ are the equivalent admittances of the positive-sequence rotor branch, the magnetizing branch and the sum of the parallel combination of the excitation capacitive reactance and the load branch with the stator winding and the negative-sequence branches. $\dot{E}_1$ is not equal to zero for the voltage building up successfully, the relationship of the following nodal admittance holds;

$$\dot{Y}_e + \dot{Y}_m + \dot{Y}_r = 0 \tag{5}$$

where $\dot{Y}_e$, $\dot{Y}_m$ and $\dot{Y}_r$ can be represented by using the equivalent circuit as follows;

$$\dot{Y}_e = \frac{1}{\frac{(\frac{R_L}{f}+jX_L)(\frac{-jX_C}{f^2})}{\frac{R_L}{f}+j(X_L-\frac{X_C}{f^2})}+(\frac{R_1}{f}+\frac{R_2}{f+v})+jX_{12}} \quad (6)$$

where $X_{12} = X_1 + X_2$

$$\dot{Y}_m = -\frac{j}{X_m} \quad (7)$$

and

$$\dot{Y}_r = \frac{1}{\left[\frac{R_2}{f-\upsilon}+jX_2\right]} \quad (8)$$

Equating the sum of the imaginary terms in eqn.(5) to zero, the magnetizing reactance can be obtained by,

$$X_m = \frac{1}{B_e + B_r} \quad (9)$$

and then equating the sum of the real terms of eqn.(5) to zero, the 13th order polynomial function in the per unit frequency f can be written by,

$$\begin{aligned} &Y_{13}f^{13}+Y_{12}f^{12}+Y_{11}f^{11}+Y_{10}f^{10}+Y_9f^9 \\ &+Y_8f^8+Y_7f^7+Y_6f^6+Y_5f^5+Y_4f^4 \\ &+Y_3f^3+Y_2f^2+Y_1f+Y_0=0 \end{aligned} \quad (10)$$

where B_e, B_r and the fourteen coefficients from Y_0 to Y_{13} are derived and given in the appendix (*i*).

Observing eqn.(10), the per-unit frequency f can be determined using Newton Raphson method and then from eqn.(9), the magnetizing reactance Xm is also estimated. The air gap rms voltage E_1 is evaluated from eqn.(3). The following equations derived from Fig.5 represent the single-phase SEIG performances. That is,
the terminal voltage of the single-phase SEIG;

$$V_L = fE_1 \frac{\left|\frac{1}{\dot{Y}_e}-\left[\frac{R_1}{f}+\frac{R_2}{f+v}+j(X_1+X_2)\right]\right|}{\left|\frac{1}{\dot{Y}_e}\right|} \quad (11)$$

The load current of the passive inductive load in stand-alone application system;

$$I_L = \frac{V_L}{\sqrt{R_L^2+f^2X_L^2}} \quad (12)$$

The active power of the passive load;

$$P_L = I_L^2 R_L \quad (13)$$

The reactive power of the passive laod;

$$Q_L = fI_L^2 X_L \quad (14)$$

3. Single-Phase SEIG Analysis based on Per-Unit Slip Frequency Variable Approach

The equations govern the steady-state operating performances of the single-phase SEIG based on the per-unit slip frequency state variable are derived from the approximate electro-mechanical equivalent circuit of the single-phase SEIG displayed in Fig.6 by applying the nodal admittance approach with a given excitation capacitor capacitance, load impedance, machine equivalent circuit parameters and the speed of the prime mover modeled by the separately-excited dc motor.

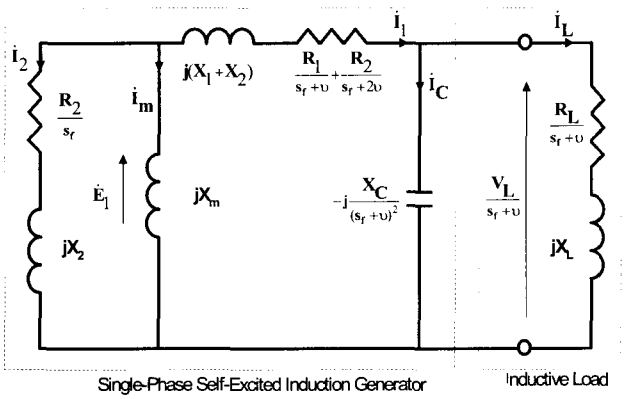

Fig. 6 Approximate electro-mechanical equivalent circuit of single-phase SEIG as a function of s_f

$\dot{Y}_e$, $\dot{Y}_m$ and $\dot{Y}_r$ can be expressed by using the above approximate electro-mechanical equivalent circuit as follows,

$$\dot{Y}_e = \frac{1}{\frac{(\frac{R_L}{s_{f\upsilon}}+jX_L)\frac{-jX_C}{s_{f\upsilon}^2}}{\frac{R_L}{s_{f\upsilon}}+j\left[X_L-\frac{X_C}{s_{f\upsilon}^2}\right]}+\frac{R_1}{s_{f\upsilon}}+\frac{R_2}{s_{f\upsilon}+\upsilon}+jX_{12}} \quad (15)$$

where $s_{f\upsilon} = s_f + \upsilon$ and s_f is the per unit slip frequency and defined as s_f=f-v.

$$\dot{Y}_m = -\frac{j}{X_m} \tag{16}$$

and

$$\dot{Y}_r = \frac{1}{\left[\frac{R_2}{s_f} + jX_2\right]} \tag{17}$$

Equating the sum of the imaginary terms in eqn.(5) to zero, the magnetizing reactance X_m can be obtained by,

$$X_m = \frac{1}{B_e + B_r} \tag{18}$$

and then equating the sum of the real terms of eqn.(5) to zero, the 5th order polynomial as a function of the per- unit slip frequency s_f can be written by,

$$Y_5 s_f^5 + Y_4 s_f^4 + Y_3 s_f^3 + Y_2 s_f^2 + Y_1 s_f + Y_0 = 0 \tag{19}$$

where B_e, B_r and the six coefficients from Y_0 to Y_5 are derived and provided in appendix(ii).

From eqn.(19), the per-unit slip frequency s_f can be determined by using Newton Raphson method and then the air gap voltage E_1 is evaluated on the basis of eqn.(3). The single-phase SEIG performances such as the generated terminal voltage of the single-phase SEIG , the load current, and the active and reactive load power can be respectively estimated by,

$$V_L = s_{f\upsilon} E_1 \frac{\left|\frac{1}{\dot{Y}_e} - \left[\frac{R_1}{s_{f\upsilon}} + \frac{R_2}{s_{f\upsilon} + \upsilon} + jX_{12}\right]\right|}{\left|\frac{1}{\dot{Y}_e}\right|} \tag{20}$$

$$I_L = \frac{V_L}{\sqrt{R_L^2 + {s_{f\upsilon}}^2 X_L^2}} \tag{21}$$

$$P_L = I_L^2 R_L \tag{22}$$

$$Q_L = s_{f\upsilon} I_L^2 X_L \tag{23}$$

4. SVC-based Voltage Regulation Scheme of Single-Phase SEIG in Parallel with Passive Load

The SVC is employed in some different power applications such as the power factor correction, the enhancement of the power system stability, the increasing of the power transfer capability of the long transmission and distribution power network lines and the voltage regulation [12]. There are different techniques employed to regulate the generated terminal voltage of the single-phase SEIG. The single-phase SVC composed of the TCR in parallel with the FC and the TSC for the generated terminal voltage regulation of the single-phase SEIG due to the passive electrical load changes as shown in Fig.7 is established herein. The conventional proportional and integrator PI controller is synthesized for controlling the equivalent excitation capacitance of the single-phase SVC.

5. SVC with PI controller for Voltage Regulation of Single-Phase SEIG

In Fig.7, the single-phase SVC composed of the TCR in parallel with the TSC and FC is implemented for the output voltage regulation of the single-phase SEIG. It is known that the control range of the triggering delayed angle α of the TCR is between $\pi/2$ and π. When the triggering delayed angles of the anti-parallel thyristors in TCR are equal to $\pi/2$ and $3\pi/2$, respectively, the anti-parallel thyristors of the zero current switching TCR are fully conduction. While the anti-parallel thyristors in the TCR are both off as the triggering delayed angles are π and 2π, respectively. Therefore, the equivalent susceptance of TCR change occurs when the triggering delayed angle α is between $\pi/2$ and π. The instantaneous current flowing through the inductor in TCR for different triggering delayed angle α is expressed by[12],

$$i_{TCR}(t) = \begin{cases} \frac{\sqrt{2}V_L}{X_{TCR}}(\cos\alpha - \cos\omega t) & \alpha \le \omega t \le \alpha + \sigma \\ 0 & \sigma + \alpha \le \omega t \le \alpha + \pi \end{cases} \tag{24}$$

where α is the thyristor triggering delayed angle with respect to zero crossing voltage waveform, σ is the conduction angle of the thyristors, X_{TCR} is the equivalent inductive reactance of TCR inductor. V_L is the effective value of the single-phase SEIG generated terminal voltage and ω is the electrical angular frequency. The fundamental component of the inductive reactor current through TCR defined previously by the above equation is obtained on the basis of using the Fourier series expansion as follows,

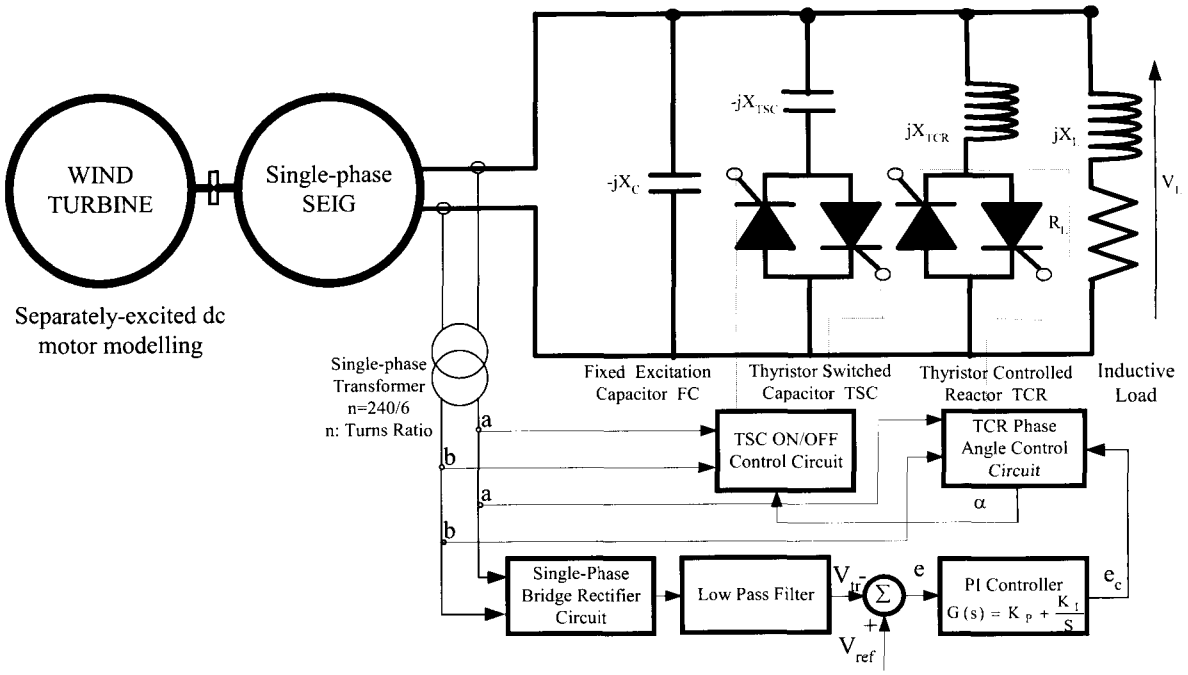

Fig. 7 A schematic system configuration of single-phase SEIG wind turbine regulated speed with SVC voltage regulation feedback closed loop scheme

$$I_{TCR1} = \frac{\sigma - \sin\sigma}{\pi X_{TCR}} V_L \tag{25}$$

where

$$\alpha + \frac{\sigma}{2} = \pi \tag{26}$$

The eqn.(25) can be conveniently written as a function of the inductive susceptance of TCR,

$$I_{RTC1} = B_{TCR}(\sigma) V_L \tag{27}$$

where B_{TCR} is an equivalent inductive susceptance of TCR and a function of the conduction angle σ (rad) and it is given by,

$$B_{TCR}(\sigma) = \frac{\sigma - \sin\sigma}{\pi X_{TCR}} \tag{28}$$

Observing the above equation, the value of inductive susceptance B_{TCR} is between $1/X_{TCR}$ and zero when σ is equal to π i.e. α is equal to $\pi/2$ and σ is equal to zero i.e. α is equal to π, respectively.

The Laplace transformation-based transfer function of the PI controller with K_P and K_I parameters in the voltage regulation feedback loop is represented by,

$$G(s) = K_P + \frac{K_I}{s} \tag{29}$$

where K_P is the proportional gain and K_I is the integral gain.

The input signal to the PI controller is also estimated by,

$$E(s) = V_{ref}(s) - V_{tr}(s) \tag{30}$$

where E(s) is the Laplace transformation of the output voltage error, $V_{ref}(s)$ is the Laplace transformation of the reference voltage $V_{ref}(t)$and $V_{tr}(s)$ is the Laplace transformation of the rectified output voltage $v_L(t)$ of the single-phase SEIG.

The Laplace transformation of the output signal of the PI controller is indicated by,

$$E_C(s) = E(s)(K_P + \frac{K_I}{s}) \tag{31}$$

The eqn.(31) can be expressed in the discrete form for the MATLAB-based simulation analysis by,

$$E_C(k) = E_C(k-1) + (K_P + T_s K_I)E(k) - K_P E(k-1) \tag{32}$$

where E(k) is the terminal voltage error signal $V_{ref}(k)$-$V_{tr}(k)$at a sampling time k, E(k-1) is the error signal at a

sampling time (k-1), T_s is the sampling period(sec) .

6. Steady-State Performances of SVC-based Voltage Regulation Feedback Scheme

As mentioned above, the equivalent susceptance B_{TCR} of the TCR controlled by the PI controller is changed on-line in order to minimize the terminal generated voltage error. The approximate electro-mechanical equivalent circuit of the single-phase SEIG with the equivalent susceptance B_{TCR} of the single-phase SVC composed of the FC in parallel with TSC and TCR which is a function of the thyristor conduction angle σ relating to the triggering delayed angle α is modified as shown in Fig.8.

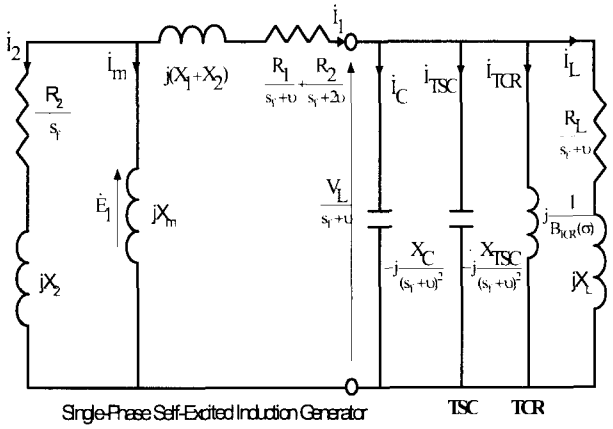

Fig. 8 Approximate electro-mechanical equivalent circuit of single-phase SEIG with SVC

Using the admittance approach with the per-unit slip frequency state variable, $\dot{Y}_e$, $\dot{Y}_m$ and $\dot{Y}_r$ can be expressed using the approximate electro-mechanical equivalent circuit represented in Fig.8,

$$\dot{Y}_e = \frac{1}{\frac{-j(X_{SVC})(\frac{R_L}{s_{f\upsilon}} + jX_L)}{\frac{R_L}{s_{f\upsilon}} + j[X_L - X_{SVC}]} + \frac{R_1}{s_{f\upsilon}} + \frac{R_2}{s_{f\upsilon}+\upsilon} + jX_{12}} \tag{33}$$

where $X_{SVC} = \dfrac{X_C + X_{TSC}}{s_{f\upsilon}^2 - (X_C + X_{TSC})B_{TCR}}$

$$\dot{Y}_m = -\frac{j}{X_m} \tag{34}$$

and

$$\dot{Y}_r = \frac{1}{\left[\frac{R_2}{s_f} + jX_2\right]} \tag{38}$$

Equating the sum of the imaginary terms in eqn.(5) to zero, the magnetizing reactance X_m can be obtained by,

$$X_m = \frac{1}{B_e + B_r} \tag{36}$$

and then equating the sum of the real terms of eqn.(5) to zero, the 7th order polynomial function with respect to the per unit slip frequency s_f can be written by,

$$\begin{aligned} &Y_7 s_f^7 + Y_6 s_f^6 + Y_5 s_f^5 + Y_4 s_f^4 + Y_3 s_f^3 \\ &+ Y_2 s_f^2 + Y_1 s_f + Y_0 = 0 \end{aligned} \tag{37}$$

where B_e, B_r and the eight coefficients from Y_0 to Y_7 are derived and provided in appendix (iii).

From eqn.(37), the per unit slip frequency s_f can be determined by using Newton Raphson method and the air gap rms voltage E_1 is then evaluated from eqn.(3). The single-phase SEIG Performances, the generated terminal voltage of the single-phase SEIG, the load current and the active and reactive load power can be respectively calculated by using,

$$V_L = s_{f\upsilon} E_1 \frac{\left|\frac{1}{\dot{Y}_e} - \left[\frac{R_1}{s_{f\upsilon}} + \frac{R_2}{s_{f\upsilon}+\upsilon} + jX_{12}\right]\right|}{\left|\frac{1}{\dot{Y}_e}\right|} \tag{38}$$

$$I_L = \frac{V_L}{\sqrt{R_L^2 + s_{f\upsilon}{}^2 X_L^2}} \tag{39}$$

$$P_L = I_L^2 R_L \tag{40}$$

$$Q_L = s_{f\upsilon} I_L^2 X_L \tag{41}$$

7. Conclusions

The present paper has introduced a novel steady-state algorithm to analyze and evaluate the single-phase SEIG performances for the stand-alone clean renewable energy utilizations in a rural alternative area, which is based on the per-unit slip frequency state variable defined newly instead

of the per-unit frequency. The essential features of the proposed power conditioner technique were that the order of the resultant equations used to find the single-phase SEIG performances are in principle reduced and then the computer software solution was very easy and simple. Moreover, the PI controller-based feedback control scheme using the single-phase SVC composed of the FC in parallel with the TCR and the TSC has implemented for the stable generated terminal voltage regulation of the single-phase SEIG loaded by different inductive loading conditions.

In the next part of this paper, a single-phase SEIG prototype setup has established for a small-scale stable wind turbine driven power conditioner with simple control strategy and the feasible experimental and simulation results in the operating performances in the steady-sate of the single-phase SEIG will be presented.

References

[1] M.Konstenko and L.Piotravsky, "Electrical Machines", Mir Publishers, Moscow, 1969.

[2] A.K.Tandon, S.S.Murthy and G.J.Berg, "Steady State Analysis of Capacitor Self-Excited Induction Generator", IEEE Trans. on Power Advances Systems, Vol. PAS-103, No.3, pp.612-618, March, 1984

[3] M.Ermis, H.B.Erton, M.Demirekler, B.M.Saribatir , Y.Uctvg, M.E.Sezer and I.Cadirici," Various Induction Generator Schemes for Wind-Electricity Generation", Electric Power Systems Research, Vol.23, pp.71-83, 1992

[4] T.F.Chan, "Analysis of Self-Excited Induction Generator Using an Iterative Method", IEEE Trans. on Energy Conversion, Vol.EC-10, No.3 PP.502-507, September 1985.

[5] Bhim Singh," Induction Generator- a Prospective", Journal of Electric Machines and Power Systems, Vol.23, pp.163-177, 1995

[6] T.F.Chan "Analysis of A Single-Phase Self-Excited Induction Generator", Journal of Electric Machines and Power Systems, Vol.23, pp.149-162, 1995.

[7] A.A.Shaltout and M.A.Adel-Halim, "Solid State Control of Wind-Driven Self-Excited Induction Generator", Electric Machines and Power Systems, Vol.23, pp.571-582, 1995

[8] S.P.Singh, M.P.Jain and Bhim Singh, "A New Technique for Analysis of Self-Excited Induction Generator", Journal of Electric Machine and Power Systems, Vol.23, pp.647-656,1995.

[9] S.Rajakarvna and R.Bonert, "A Technique for The Steady state Analysis of Self-Excited Induction Generator with variable speed", IEEE Trans. on Energy Conversion, Vol.10, No.1 pp.10-16, March, 1995.

[10] W. Koczara, " Variable Speed Three-Phase Power Generation Set", CD-Rom, EPE-2001, 2001.

[11] A. Koyanagi," Maximum Power Point Tracking of Wind Turbine Generator Using a Flywheel", Proceedings of the 2001 Japan Industry Application society Conference, Vol.1, pp.395-398, 2001.

[12] IEEE Special Stability Controls Working Group Report, "Static VAR Compensator Models for Power Flow and Dynamic Performance Simulation ", IEEE Trans. on Power Systems, Vol.9, No.1, February 1994.

Appendix(i)

$$B_e = \frac{X_e}{R_e^2 + X_e^2}$$

where

$$R_e = \frac{B_5 f^5 + B_4 f^4 + B_3 f^3 + B_2 f^2 + B_1 f + B_0}{(A_5 f^5 + A_4 f^4 + A_3 f^3 + A_2 f^2 + A_1 f + A_0) f}$$

and

$$X_e = \frac{(C_5 f^5 + C_4 f^4 + C_3 f^3 + C_2 f^2 + C_1 f + C_0) f}{(A_5 f^5 + A_4 f^4 + A_3 f^3 + A_2 f^2 + A_1 f + A_0) f}$$

$A_0=\upsilon X^2_C$, $A_1=X^2_C$, $A_2=\upsilon\,(R_L{}^2-2X_LX_C)$, $A_3=R_L{}^2-2X_LX_C$,

$A_4=\upsilon X_L{}^2$, $A_5=X_L{}^2$,

$B_0=\upsilon A_1(R_1+R_L)$, $B_1=A_1(R_1+R_2+R_L)$, $B_2=\upsilon R_1A_3$,

$B_3=(R_1+R_2)A_3$, $B_4=\nu R_1A_5$, $B_5=(R_1+R_2)A_5$,

$C_0=\upsilon(X_CR_L{}^2-X_LX_C{}^2-X_{12}A_1)$, $C_1=X_CR_L{}^2-X_LX_C{}^2-X_{12}A_1$,

$C_2=\upsilon(X_CX_L{}^2-X_{12}A_3)$, $C_3=X_CX_L{}^2-X_{12}A_3$, $C_4=-\upsilon X_{12}A_5$,

$C_5=-X_{12}A_5$, $X_{12}=X_1+X_2$

$$B_r = -\frac{(f-\upsilon)^2 X_2}{R_2^2 + (f-\upsilon)^2 X_2^2}$$

$Y_0=-\upsilon R_2G_0$, $Y_1=R_2G_0-\upsilon R_2G_1+E_0O_0$,

$Y_2=R_2G_1-\upsilon R_2(G_2+H_0)+E_1O_1+E_0O_2$,

$Y_3=R_2(G_2+H_0)-\upsilon R_2(G_3+H_1)+E_2O_1+E_1O_2+E_0O_3$,

$Y_4=R_2(G_3+H_1)-\upsilon R_2(G_4+H_2)+E_2O_2+E_1O_3+E_0O_4$,

$Y_5=R_2(G_4+H_2)-\upsilon R_2(G_5+H_3)+E_2O_3+E_1O_4+E_0O_5$

$Y_6=R_2(G_5+H_3)-\upsilon R_2(G_6+H_4)+E_2O_4+E_1O_5+E_0O_6$,

$Y_7=R_2(G_6+H_4)-\upsilon R_2(G_7+H_5)+E_2O_5+E_1O_6+E_0O_7$,

$Y_8=R_2(G_7+H_5)-\upsilon R_2(G_8+H_6)+E_2O_6+E_1O_7+E_0O_8$,

$Y_9=R_2(G_8+H_6)-\upsilon R_2(G_9+H_7)+E_2O_7+E_1O_8+E_0O_9$,

$Y_{10}=R_2(G_9+H_7)-\upsilon R_2(G_{10}+H_8)+E_2O_8+E_1O_9+E_0O_{10}$,

$Y_{11}=R_2(G_{10}+H_8)-\upsilon R_2H_9+E_2O_9+E_1O_{10}+E_0O_{11}$,

$Y_{12}=R_2H_9-\upsilon R_2H_{10}+E_2O_{10}+E_1O_{11}$, $Y_{13}=R_2(H_{10})+E_2O_{11}$

where, $O_1=B_0A_0$, $O_2=B_1A_0+B_0A_1$,$O_3=B_2A_0+B_1A_1+B_0A_2$,
$O_4=B_3A_0+B_2A_1+B_1A_2+B_0A_3$,
$O_5=B_4A_0+D_3L_1+D_2L_2+D_1L_3+D_0L_4$,
$O_6=B_5A_0+B_4A_1+B_3A_2+B_2A_3+B_1A_4+B_0A_5$,
$O_7=B_5A_1+B_4A_2+B_3A_3+B_2A_4+B_1A_5$,
$O_8=B_5A_2+B_4A_3+B_3A_4+B_2A_5$, $O_9=B_5A_3+B_4A_4+B_3A_5$,
$O_{10}=B_5A_4+B_4A_5$, $O_{11}=B_5A_5$,
$G_0=B_0^2$, $G_1=2B_1B_0$, $G_2=2B_2B_0+B_1^2$,$G_3=2B_3B_0+2B_2B_1$,
$G_4=2B_4B_0+2B_3B_1+B_2^2$, $G_5=2B_5B_0+2B_4B_1+2B_3B_2$,
$G_6=2B_5B_1+2B_4B_2+B_3^2$, $G_7=2B_5B_2+2B_4B_3$,
$G_8=2B_5B_3+B_4^2$, $G_9=2B_5B_4$, $G_{10}=B_5^2$,
$H_0=C_0^2$, $H_1=2C_1C_0$, $H_2=2C_2C_0+C_1^2$, $H_3=2C_3C_0+2C_2C_1$,
$H_4=2C_4C_0+2C_3C_1+C_2^2$, $H_5=2C_5C_0+2C_4C_1+2C_3C_2$,
$H_6=2C_5C_1+2C_4C_2+C_3^2$, $H_7=2C_5C_2+2C_4C_3$,
$H_8=2C_5C_3+C_4^2$, $H_9=2C_5C_4$, $H_{10}=C_5^2$,
$E_0=R_2^2+\upsilon^2X_2^2$, $E_1=-2\upsilon X_2^2$, $E_2=X_2^2$,

Appendix (ii)

$$B_e=(s_f+\upsilon)\frac{X_e}{R_e^2+X_e^2}$$

where $$R_e=\frac{B_2s^2+B_1s+B_0}{A_1s+A_0}$$

and $$X_e=\frac{C_2s^2+C_1s+C_0}{A_1s+A_0}$$

Assuming that, s_f^2 is neglected with respect to υ^2
$A_0=X^2_C+\upsilon^2R_L^2+\upsilon^4X_L^2-2\upsilon^2X_LX_C$
$A_1=2\upsilon R_L^2+4\upsilon^3X_L^2-4\upsilon X_LX_C$,
$R_{12}=R_2/2\upsilon$, $R_{22}=R_1+R_2/2$,
$B_0=R_{22}A_0+R_LX_C^2$, $B_1=R_{22}A_1+R_{12}A_0$, $B_2=R_{12}A_1$
$D_0=R_L^2X_C+\upsilon^2X_L^2X_C-X_LX_C^2$, $D_1=2\upsilon X_L^2X_C$
$X_{12}=X_1+X_2$, $C_0=\upsilon(D_0-X_{12}A_0)$,
$C_1=D_0+\upsilon(D_1-X_{12}A_1)-X_{12}A_0$, $C_2=D_1-X_{12}A_1$

$$B_r=-\frac{s_f^2X_2}{R_2^2}$$

Assuming that, $s_f^2X_2^2$is neglected with respect to R_2^2
$O_0=A_0B_0$, $O_1=A_0B_1+A_1B_0$, $O_2=A_0B_2+A_1B_1$, $O_3=A_1B_2$
$G_0=B_0^2$, $G_1=2B_1B_0$, $G_2=2B_2B_0+B_1^2$, $G_3=2B_1B_2$, $G_4=B_2^2$,
$Y_0=Q_0$, $Y_1=Q_1+H_0+G_0$, $Y_2=Q_2+H_1+G$, $Y_3=Q_3+H_2+G_2$,
$Y_4=Q_4+H_3+G_3$, $Y_5=H_4+G_4$
Where,
$H_0=C_0^2$, $H_1=2C_1C_0$, $H_2=2C_2C_0+C_1^2$, $H_3=2C_1C_2$, $H_4=C_2^2$,
$Q_0=\upsilon R_2O_0$, $Q_1=R_2(\upsilon O_1+O_0)$, $Q_2=R_2(\upsilon O_2+O_1)$,
$Q_3=R_2(\upsilon O_3+O_2)$, $Q_4=R_2O_3$

Appendix (iii)

$$B_e=(s_f+\upsilon)\frac{X_e}{R_e^2+X_e^2}$$

where, $$R_e=\frac{D_3s_f^3+D_2s_f^2+D_1s_f+D_0}{A_2s_f^2+A_1s_f+A_0}$$

and $$X_e=\frac{C_3s_f^3+C_2s_f^2+C_1s_f+C_0}{A_2s_f^2+A_1s_f+A_0}$$

$A_0=X_{C3}^2+b_C^2R_L^2$, $A_1=2b_CR_L^2+2X_{C3}$, $A_2=X_{C4}^2$, $X_{C1}=X_C/2$,

$$b_c=\frac{\upsilon}{2}-\frac{X_C(\sigma-\sin\sigma)}{2\pi\upsilon X_R}$$

$$X_{C2}=\frac{X_C}{2\upsilon}$$, $X_{C3}=\upsilon b_CX_L-X_{C1}$, $X_{C4}=(\upsilon+b_C)X_L-X_{C2}$,

$X_{12}=X_1+X_2$, $C_0=B_0-\upsilon X_{12}A_0$, $C_1=B_1-\upsilon X_{12}A_1-X_{12}A_0$,
$C_2=B_2-X_{12}A_1-X_{12}A_1$, $C_3=-X_{12}A_2$,
$B_0=b_CR_L^2X_{C1}+\upsilon X_{c1}X_{C3}X_L$,
$B_1=R_L^2(b_CX_{C2}+X_{C1})+X_L(\upsilon X_{C2}X_{C3}+\upsilon X_{C1}X_{C4}+X_{C1}X_{C3})$,
$B_2=R_L^2X_{C2}+X_L(\upsilon X_{C2}X_{C4}+X_{C1}X_{C4}+X_{C2}X_{C3})$,
$R_{12}=R_2/2\upsilon$, $R_{22}=R_1+R_2/2$,
$D_0=R_{22}A_0+F_0$, $D_1=R_{22}A_1+R_{12}A_0+F_1$,
$D_2=R_{22}A_2+R_{12}A_1+F_2$, $D_3=R_{12}A_2$, $F_0=X_{C1}^2R_L$,
$F_1=2X_{C2}X_{C1}R_L$, $F_2=X_{C2}^2R_L$,

$$B_r=-\frac{s_f^2X_2}{R_2^2}$$

$Y_0=Q_0$, $Y_1=Q_1+H_0+G_0$, $Y_2=Q_2+H_1+G_1$, $Y_3=Q_3+H_2+G_2$,
$Y_4=Q_4+H_3+G_3$, $Y_5=Q_5+H_4+G_4$, $Y_6=Q_6+H_5+G_5$,
$Y_7=H_6+G_6$
Where, $O_0=D_0A_0$, $O_1=D_1A_0+D_0A_1$,
$O_2=D_2A_0+D_1A_1+D_0A_2$, $O_3=D_3A_0+D_2A_1+D_1A_2$,
$O_4=D_3A_1+D_2A_2$, $O_5=D_3A_2$, $G_0=D_0D_0$, $G_1=D_1D_0+D_0D_1$,
$G_2=D_2D_0+D_1D_1+D_0D_2$, $G_3=D_3D_0+D_2D_1+D_1D_2+D_3D_0$,
$G_4=D_3D_1+D_2D_2+D_1D_3$, $G_5=D_3D_2+D_2D_3$, $G_6=D_3D_3$,
$H_0=C_0C_0$, $H_1=C_1C_0+C_0C_1$, $H_2=C_2C_0+C_1C_1+C_0C_2$,
$H_3=C_3C_0+C_2C_1+C_1C_2+C_0C_3$, $H_4=C_3C_1+C_2C_2+C_1C_3$,
$H_5=C_3C_2+C_2C_3$, $H_6=C_3C_3$, $E_0=\upsilon R_2$, $E_1=R_2$,
$Q_0=O_0E_0$, $Q_1=O_1E_0+O_0E_1$, $Q_2=O_2E_0+O_1E_1$,
$Q_3=O_3E_0+O_2E_1$, $Q_4=O_4E_0+O_3E_1$, $Q_5=O_5E_0+O_4E_1$,
$Q_6=O_5E_1$

Tarek Ahmed
He received his M Sc.-Eng from the Electrical Engineering Department, Assiut University, Egypt in 1998. He is currently a Ph. D. candidate student in the Graduate School of Science and Engineering, the Power Electronic System and Control Engineering Laboratory at Yamaguchi University, Yamaguchi, Japan. His research interests are in the area of the new applications for the power electronic circuits and systems with the renewable energy and power systems and semiconductor power conditioners. Mr. Ahmed is a student-member of the IEEE and the Japan Society of the Power Electronics.
Tel: +81-836-85-9472, Fax: +81-836-85-9401

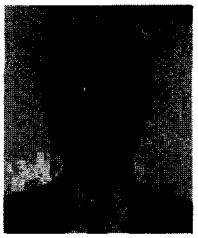

Osamu Noro
He received his M. Sc. in Applied Mathematics and Physics from Kyoto University, Kyoto, Japan. He is currently the manager of the Power Electronic Section, Development Department-1, System Technology Development Center of Kawasaki Heavy Industries Ltd., Akashi, Japan. His research interests are in the applications of systems technology consisting of the power electronics and electric machines such as turbine generator system, motor drive, electric and mechanical power conversion systems and so on. He is a member of IEEE and the Japan Society of Mechanical Engineers.

Koji Soshin
He received his M.Sc.-Eng from the Electronic Engineering Department, the Graduate School of Electrical and Electronics Engineering,. Kobe University, Kobe, Japan. He joined Matsushita Electric Works, Ltd. in 1979. He is interested in stepping motor applications, vector controlled inverter for the induction motor and power electronic circuits and systems technologies. He are now working in the power supplies for electric vehicle. He is now a Ph. D. candidate student in the Graduate School of Science and Engineering, Yamaguchi University, Yamaguchi, Japan. Mr. Soshin is a member of the Japan Society of Power Electronics.

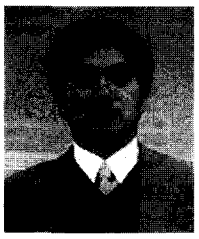

Shinji Sato
He graduated from Mechanical Engineering, Technical Collage of Nigata East High School. He joined in the research project at Toshiba Corporation, Tokyo. After that, he joined in research and development of Sanken Electric, Co. Ltd. Saitama. He is now studying in the Power Electronic System Laboratory, the Graduate School of Science and Engineering, Yamaguchi University, Yamaguchi, Japan. His research area includes the soft-switching PWM rectifiers and DC-DC converters. He received the 2002 paper award in IEE-IAS-Japan. He is a member of Japan Society of System, Information and Control Engineers and Japan Society of Power Electronics.

Eiji Hiraki
He received his M. Sc.-Eng in Electrical Engineering from Osaka University, Osaka, Japan in 1990. He is currently with the Power Electronic System and Control Engineering Laboratory at Yamaguchi University, Yamaguchi, Japan, as a Research Associate. His research interests are in the soft-switching technique for high frequency switching power conversion systems. Mr. Hiraki is a member of IEE-Japan, the Japan Society of the Power Electronics and IEEE.

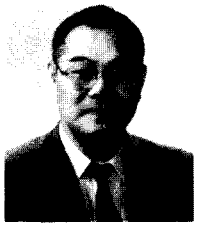

Mutsuo Nakaoka
He received his Dr-Eng. degree in Electrical Engineering from Osaka University, Osaka, Japan in 1981. He joined the Electrical and Electronics Engineering Department of Kobe University, Kobe, Japan in 1981. Since 1995, he has been a professor of the Electrical and Electronics Engineering Department, the Graduate School of Science and Engineering, Yamaguchi University, Yamaguchi, Japan. His research interests include application developments of power electronics circuit and systems. He received the 2001 premium paper award from IEE-UK and so on. Dr. Nakaoka is a member of the Institute of Electronics, Information and Communication Engineers of Japan, Institute of Illumination Engineering of Japan, European Power Electronics Association, the Japan Society of the Solar Energy, IEE-Korea and IEEE.